

# Variable-Complexity Response Surface Design of an HSCT Configuration\*

Anthony A. Giunta<sup>†</sup>      Vladimir Balabanov<sup>†</sup>      Matthew Kaufman<sup>†</sup>  
Susan Burgee<sup>§</sup>      Bernard Grossman<sup>¶</sup>      Raphael T. Haftka<sup>‡</sup>  
William H. Mason<sup>#</sup>      Layne T. Watson<sup>\*\*</sup>

## Abstract

A variable-complexity response surface methodology has been applied to the multidisciplinary design of a High Speed Civil Transport (HSCT). The term *variable-complexity* refers to a design procedure in which refined, computationally expensive analysis techniques are combined with simple, computationally inexpensive techniques. We have used the simple analysis methods to define a subregion of the design space in which an optimal HSCT design is likely to exist. The refined analysis methods were then used to construct smooth response surface models of various aerodynamic and structural weight quantities. Aerodynamic response surface models were constructed for volumetric wave drag and supersonic drag due to lift based on an example problem involving four HSCT wing design variables. Optimization was then performed for the complete HSCT configuration using the aerodynamic response surface models. Preliminary research on the development of a structural response surface model for the wing bending material weight is also described. In addition to the results for the variable-complexity response surface modeling and optimization, performance data are presented for a coarse grained parallelization of the aerodynamic and structural analyses.

## 1 Introduction

The use of multidisciplinary optimization techniques in aerospace vehicle design often is limited because of the significant computational expense incurred in the analysis of the vehicle and its many systems. In response to this difficulty, a variable-complexity modeling approach, involving the use of refined and computationally expensive models together with simple and computationally inexpensive models has been developed. This variable-complexity technique has been previously applied to the combined aerodynamic-structural optimization of subsonic transport aircraft wings [26] and the aerodynamic-structural optimization of the High Speed Civil Transport (HSCT) [8], [22].

In related research conducted by members of the Multidisciplinary Analysis and Design (MAD) Center for Advanced Vehicles at Virginia Tech, several improved HSCT designs have

---

\* This work was supported by NASA Grant NAG-1-1562.

<sup>†</sup> Research Assistant, Dept. of Aerospace & Ocean Eng., Virginia Tech, Blacksburg, VA 24061.

<sup>§</sup> Research Assistant, Dept. of Computer Science, Virginia Tech, Blacksburg, VA 24061-0106.

<sup>¶</sup> Professor & Dept. Head, Dept. of Aerospace & Ocean Eng., Virginia Tech, Blacksburg, VA 24061.

<sup>‡</sup> Professor, Dept. of Aero. Eng., Mech. & Eng. Sci., University of Florida, Gainesville, FL 32611-6250.

<sup>#</sup> Professor, Dept. of Aerospace & Ocean Eng., Virginia Tech, Blacksburg, VA 24061.

<sup>\*\*</sup> Professor, Depts. of Computer Sci. and Math., Virginia Tech, Blacksburg, VA 24061-0106.

been obtained using these multidisciplinary design optimization tools. However, these efforts were hindered by convergence difficulties which were encountered in the aerodynamic–structural optimization of the HSCT [12]. The convergence problems were traced to numerical noise which inhibited the use of gradient-based optimization techniques. To address this problem, a two variable example problem was investigated in which response surface models were used to produce smooth approximations for drag due to lift, a quantity affected by numerical noise [12]. This example problem was used to determine the feasibility of using response surface methodology in conjunction with our existing multidisciplinary analysis tools. Such applications of response surface methods to vehicle design were proven successful by other investigators, see [10] and [15].

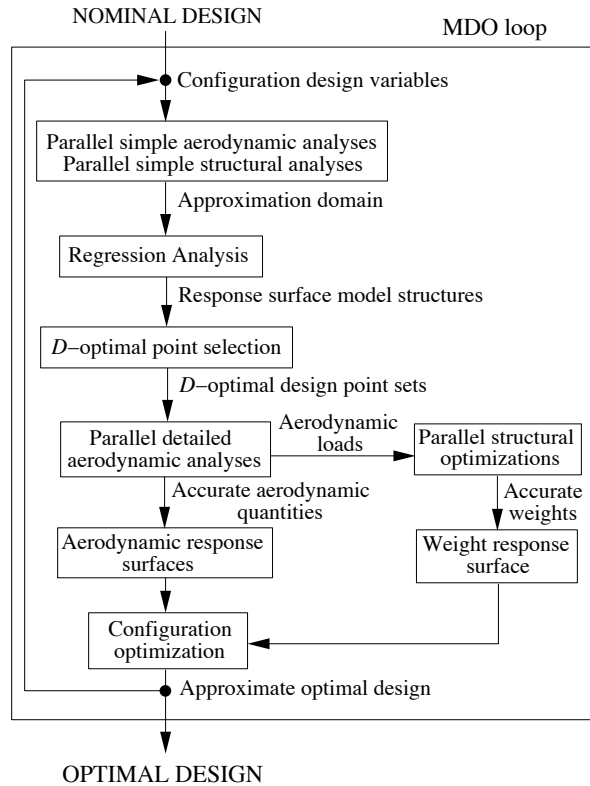


Figure 1. General flow chart for HSCT design.

This study focuses on applying a variable-complexity response surface approximation strategy to HSCT design optimization. The simple analysis methods are used to define a subregion of the design space, i.e., the *approximation domain*, in which an optimal HSCT design is likely to exist. The refined analysis methods are then used to construct smooth response surface models of various aerodynamic and structural weight quantities which are susceptible to numerical noise. Aerodynamic response surface models were constructed for volumetric wave drag and supersonic drag due to lift for an example wing design problem involving four of the twenty-eight HSCT design variables. A structural response surface model was also investigated for the wing bending material weight factor for a problem involving twenty-five of the HSCT design variables.

The objective of the optimization procedure is to minimize the gross takeoff weight of the vehicle subject to numerous geometric, aerodynamic and performance constraints. Additional constraints limit the scope of the design space to the region over which the

response surface models are valid. Currently, the aerodynamic response surface models have been incorporated into the optimization strategy. However, we have not yet implemented the structural response surface models into this framework. A flow chart illustrating the HSCT design process is given in Figure 1.

## 2 Variable-Complexity Modeling

We have termed “variable-complexity modeling” the design process by which simple, computationally inexpensive analysis techniques are used together with more detailed, expensive techniques. Originally, this methodology was developed for gradient-based optimization in which the overall design process was composed of a sequence of optimization cycles. With this method, the detailed analyses were employed at the beginning of each optimization cycle while the simple analyses, scaled to match the initial detailed results, were performed in subsequent calculations during each cycle [8], [22]. A typical HSCT design optimization requires approximately twenty cycles until an optimal HSCT configuration is identified. The optimizer NEWSUMT-A [13], which employs an extended interior penalty function method, is used for this sequential approximate optimization process.

In the present work, this variable-complexity modeling approach is adapted for use with response surface approximation techniques. Here, the simple analysis methods are used to evaluate thousands of different HSCT configurations within a prescribed design space. By applying constraints to the design variables and to the objective function data, “nonsense” regions of the design space are excluded. The valid design space is characterized by an irregularly shaped region which contains the optimal HSCT configuration.

Using a large number of points which span the valid, but irregularly shaped, design space, a small number of points, on the order of fifty to one hundred, are then selected for more detailed analyses. Using the results from these detailed analyses, response surface approximations can be created to model various factors which affect the HSCT design. For example, drag component data from the detailed analyses can be used to create a polynomial response surface model for the variation in drag. In the final step of this process, the response surface models are implemented in the HSCT analysis software, and configuration optimization is carried out. This optimization uses constraints based on both the simple and detailed analyses, along with constraints which limit the design variables to values for which the response surface model is accurate.

## 3 Response Surface Methods

### 3.1 Polynomial Modeling

Response surface methodology (RSM) is a statistical technique in which smooth functions, typically polynomials, are used to model an objective function. For example, a quadratic response surface model for  $p$  design variables has the form:

$$(1) \quad y = c_o + \sum_{1 \leq i \leq p} c_i x_i + \sum_{1 \leq i \leq j \leq p} c_{ij} x_i x_j + \delta,$$

where the  $x_i$  are the design variables, the  $c_i$  are the polynomial coefficients,  $y$  is the measured response, and  $\delta$  is a random error term. In such a model the polynomial coefficients may be estimated using the method of least squares.

The construction of a response surface requires a minimum of  $n$  function evaluations where  $n$  is the number of coefficients in the polynomial. Results from [12] confirmed that

typically  $1.5n$  function analyses were required to produce response surfaces which accurately approximated the global trends of the objective function data.

An example of the use of response surface modeling techniques is provided in [12] where supersonic drag due to lift of an HSCT wing was calculated for various inboard leading-edge and inboard trailing-edge sweep angles. Here, drag due to lift is calculated as

$$C_{D_{lift}} = \left( \frac{1}{C_{L\alpha}} - k_t \frac{C_T}{C_L^2} \right) C_L^2, \quad (2)$$

where  $C_{L\alpha}$  is the lift curve slope,  $C_T/C_L^2$  is the leading-edge thrust term, and  $k_t$  is an attainable leading-edge thrust factor. Numerical noise in the evaluation of drag due to lift (Fig. 2) may be attributed to noise in the lift curve slope and leading-edge thrust terms. The methods of Carlson et al. [5], [6], [7] utilize a paneling scheme that is sensitive to planform changes. Thus, slight modifications to the leading and trailing-edge sweep angles, along with changes in the location where the Mach angle intersects the leading-edge, produce discontinuous variations in the predicted drag. Although the variations are small enough so that at all points the accuracy of the drag is acceptable, the oscillatory behavior creates difficulties for gradient-based optimization techniques. Nonsmooth behavior of an objective function was also encountered in a nozzle design problem [25] in which an Euler flow solver was employed indicating noisy or nonsmooth behavior is not solely related to the use of panel methods.

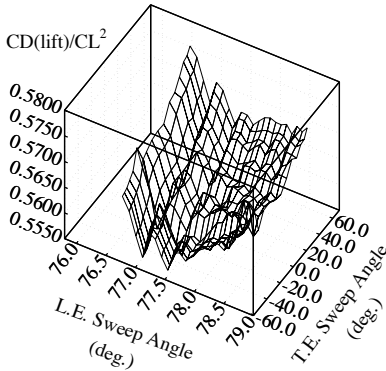


Figure 2. Noisy drag due to lift.

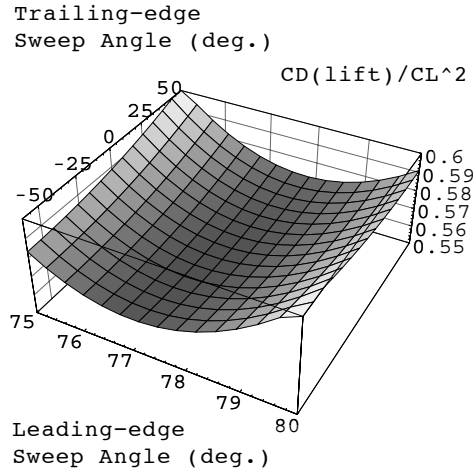


Figure 3. Quadratic polynomial response surface fit to the noisy drag due to lift data.

Figure 3 demonstrates the use of a quadratic polynomial response surface to approximate the noisy drag due to lift in Figure 2. The global minimum on the exact, noisy surface occurs for a leading-edge sweep angle of  $77.6^\circ$  and a trailing-edge sweep angle of  $-20.0^\circ$ . As shown in Figure 3, the quadratic response surface provides a reasonable estimation for the location of the global minimum.

### 3.2 D-optimal Point Selection

RSM typically employs a structured method such as central composite design (CCD) for selecting analysis points in the design space [23]. However, CCD is meant for use with regularly shaped design spaces and not the irregularly shaped design spaces that will arise in this design problem. Further, CCD is not a practical point selection method for design problems with a large number of variables. In a previous study [12], it was found that the  $D$ -optimal criterion [3] provided a rational means for choosing any number of points within an irregularly shaped design space.

The  $D$ -optimal criterion arises from the linear model  $Y \approx \mathbf{X}c$ , where  $Y$  is an  $m$  by 1 vector of objective function values,  $c$  is a  $k$  by 1 vector of coefficients to be estimated, and  $\mathbf{X}$  is an  $m$  by  $k$  matrix of constants having rank  $k$ . The rows of the matrix  $\mathbf{X}$  are the response surface basis functions evaluated at the design points. For this system, the least squares estimate of  $c$  is  $\hat{c} = (\mathbf{X}^T\mathbf{X})^{-1}\mathbf{X}^TY$ . The goal is to find the  $m$  points from a set of  $l > m$  candidate points existing in the design space that will yield the best fidelity between the polynomial model and the actual objective function. The  $D$ -optimality criterion states that the  $m$  points to choose are those which maximize the determinant  $|\mathbf{X}^T\mathbf{X}|$ . Several relevant properties of this criterion are:

1. the set of points that maximizes  $|\mathbf{X}^T\mathbf{X}|$  is also the set of points that minimizes the maximum variance of any predicted value of the objective function,
2. the set of points that maximizes  $|\mathbf{X}^T\mathbf{X}|$  is also the set of points that minimizes the variance of the parameter estimates,
3. the design obtained is invariant to changes in scale.

There are  $\binom{l}{m} = l!/(m!(l-m)!)$  combinations of  $m$  points from the set of  $l$  candidate points which is often a very large number. For example, a small problem in two design variables may be to pick twenty-five points from 121 possible points (discretizing the design domain into ten sections in both directions leads to an  $11 \times 11$  mesh). This leads to a total of  $5.26 \cdot 10^{25}$  possible combinations, one or more of which are  $D$ -optimal. Because of the large number of combinations, a genetic algorithm was developed to efficiently find a set of  $D$ -optimal points. In addition, the genetic algorithm allows  $D$ -optimal point selection for a design space of arbitrary shape.

### 3.3 Regression Analysis and ANOVA

When using RSM the designer often encounters what has been termed the “curse of dimensionality” in which the number of analysis points needed to construct a response surface model greatly increases as the number of design variables becomes large. For this reason, it would be advantageous if less significant terms in the response surface model could be eliminated.

Fortunately, there is a statistical technique, analysis of variance (ANOVA), which enables the less significant terms in the polynomial approximation to be identified. ANOVA involves estimating the variance of the predicted polynomial coefficients and uses the variance-covariance matrix  $(\mathbf{X}^T\mathbf{X})^{-1}$ . The diagonal terms in this square matrix,  $\sigma_i^2$ , multiplied by  $\text{Var}(\delta)$ , the variance in the objective function values  $Y_i$ , are the variances of the respective coefficients,  $c_i$ , in the response surface polynomial model. The coefficient of variation,  $V$ , for each term in the polynomial is calculated as

$$(2) \quad V = \begin{cases} \frac{100|\sigma_i|\sqrt{\text{Var}(\delta)}}{c_i}, & c_i \neq 0, \\ 100, & c_i = 0, \end{cases}$$

where the factor of 100 expresses the coefficient of variation as a percentage. The term  $\text{Var}(\delta)$  is usually estimated by the RMS error of the least squares approximation at the  $m$  data points. A common approximation for this term is:

$$(3) \quad \text{Var}(\delta) = E_{RMS}^2 m / (m - n),$$

where  $m$  is the number of points used in the least squares method,  $n$  is the number of terms in the model equation, and  $E_{RMS}$  is the RMS error calculated using the difference between the response of the model equation and the data used for the least squares problem.

#### 4 HSCT Design Problem

Successful aircraft configuration optimization requires a simple, yet meaningful mathematical characterization of the geometry. We have developed a model that completely defines the HSCT design problem using twenty-eight design variables. Twenty-five of the design variables describe the geometry of the aircraft and can be divided into five categories: wing planform, airfoil shape, tail areas, nacelle placement, and fuselage shape. The wing planform is described using the root and tip chord lengths, the wing span, and by blending linear line segments at the leading and trailing edges. The wing planform geometry is depicted in Figure 4. The airfoil sections have round leading edges and are defined using an analytic description incorporating the following four design variables: the location of maximum thickness-to-chord ( $t/c$ ) ratio for all airfoil sections, and the  $t/c$  ratios at the root chord, leading-edge break, and tip chord.

The horizontal and vertical tail areas are described by two variables. The nacelles are fixed along the trailing-edge of the wing with a twenty-five percent overhang, and two variables define their spanwise locations. The axisymmetric fuselage requires eight variables to specify both the axial positions and radii of the four fuselage restraint locations. Details of the geometry specification appear in References [19] and [21] and the design variables are listed in Table 1.

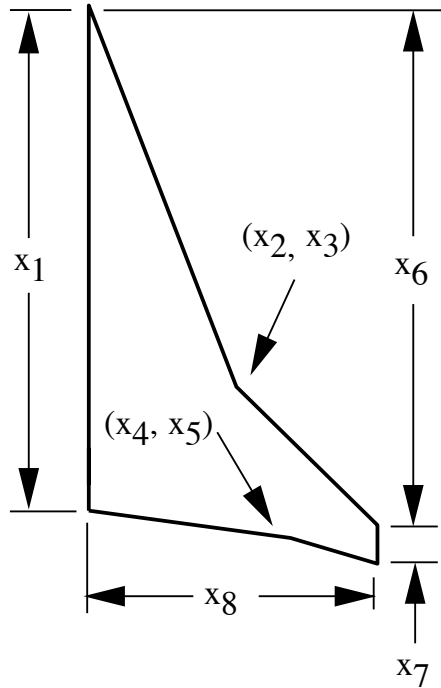


Figure 4. Planform variable definition for the HSCT wing.

Table 1. HSCT design variables and baseline values.

Num.	Value	Description	Num.	Value	Description
1	181.48	Wing root chord, ( <i>ft</i> )	15	1.06	Fuselage restraint 1, <i>r</i> ( <i>ft</i> )
2	155.9	LE break point, <i>x</i> ( <i>ft</i> )	16	12.20	Fuselage restraint 2, <i>x</i> ( <i>ft</i> )
3	49.2	LE break point, <i>y</i> ( <i>ft</i> )	17	3.50	Fuselage restraint 2, <i>r</i> ( <i>ft</i> )
4	181.6	TE break point, <i>x</i> ( <i>ft</i> )	18	132.46	Fuselage restraint 3, <i>x</i> ( <i>ft</i> )
5	64.2	TE break point, <i>y</i> ( <i>ft</i> )	19	5.34	Fuselage restraint 3, <i>r</i> ( <i>ft</i> )
6	169.5	LE wing tip, <i>x</i> ( <i>ft</i> )	20	248.67	Fuselage restraint 4, <i>x</i> ( <i>ft</i> )
7	7.00	Wing tip chord, ( <i>ft</i> )	21	4.67	Fuselage restraint 4, <i>r</i> ( <i>ft</i> )
8	75.9	Wing semi-span, ( <i>ft</i> )	22	26.23	Nacelle 1, <i>y</i> ( <i>ft</i> )
9	0.40	Chordwise max. <i>t/c</i> location	23	32.39	Nacelle 2, <i>y</i> ( <i>ft</i> )
10	3.69	LE radius parameter	24	322,617	Mission fuel, ( <i>lbs</i> )
11	2.58	Airfoil <i>t/c</i> at root, (%)	25	64,794	Starting cruise altitude, ( <i>ft</i> )
12	2.16	Airfoil <i>t/c</i> at LE break, (%)	26	33.90	Cruise climb rate, ( <i>ft/min</i> )
13	1.80	Airfoil <i>t/c</i> at tip, (%)	27	697.9	Vertical tail area, ( <i>ft</i> <sup>2</sup> )
14	2.20	Fuselage restraint 1, <i>x</i> ( <i>ft</i> )	28	713.0	Horizontal tail area, ( <i>ft</i> <sup>2</sup> )

The design problem is to minimize the takeoff gross weight of an HSCT configuration with a range of 5,500 nautical miles and a cruise speed of Mach 2.4 while transporting 250 passengers. For this mission, in addition to the geometric parameters, three variables define the idealize cruise mission (Table 1). One variable is the mission fuel and the other two are initial cruise altitude and the constant climb rate used in the range calculation.

In this study, a baseline HSCT is used for comparison purposes and to provide a rough approximation to the center of the feasible design space. The baseline geometry is from an optimal HSCT configuration previously investigated by members of our research group at Virginia Tech (Table 1) [8].

Table 2. Constraints on the HSCT design.

Num.	Geometric Constraint	Num.	Aero. & Perform. Constraint
1	Fuel volume $\leq$ 50% wing volume	35	Range $\geq$ 5,500 <i>nmi</i>
2	Spike prevention	36	$C_L$ at landing speed $\leq$ 1
3-20	Wing chord $\geq$ 7.0 <i>ft</i>	37-55	Section $C_l$ at landing speed $\leq$ 2
21	LE break $\leq$ semi span	56	Landing angle of attack $\leq$ $^{\circ}12^{\circ}$
22	TE break $\leq$ semi span	57-60	Engine scrape at landing
23	Inboard TE sweep $>$ 0 <i>deg</i>	61	Wing tip scrape at landing
24	Root chord <i>t/c</i> $>$ 1.5%	62	Rudder deflection $\leq$ 22.5 $^{\circ}$
25	LE break chord <i>t/c</i> $>$ 1.5%	63	Bank Angle $\leq$ 5 $^{\circ}$
26	Tip chord <i>t/c</i> $>$ 1.5%	64	Tail deflect. for approach $\leq$ 22.5 $^{\circ}$
27-31	Fuselage restraints, <i>x</i> , in order	65	Takeoff rotation to occur $\leq$ $V_{min}$
32	Nacelle 1 outboard of fuselage	66	Engine-out limit with vertical tail
33	Nacelle 1 inboard of nacelle 2		
34	Nacelle 2 inboard of semi-span		

Sixty-six constraints which include geometry, performance, and aerodynamic constraints are included in the optimization [8]. The aerodynamic and performance constraints can only be assessed after a complete analysis of the HSCT design; however, the geometric constraints can be evaluated using algebraic relations based on the twenty-eight design

variables. For this reason, they offer an efficient means of narrowing the feasible design space. The geometric, performance and aerodynamic constraints are listed in Table 2.

## 5 Four Design Variable Aerodynamic Design of the HSCT Wing

The detailed aerodynamic analyses use the Harris program for the supersonic volumetric wave drag [14], a Carlson Mach-box type method for supersonic drag-due-to-lift [6], [7], and a vortex-lattice program for landing performance. As part of our variable-complexity modeling approach we also employ simple aerodynamic analysis methods which are typically algebraic relations, and which require at least an order of magnitude less computational time than the associated detailed analysis methods. Details of each calculation are given in [21]. Compared to modern computational fluid dynamics tools, the detailed and simple analysis models used in this study are relatively inexpensive. However, the computational expense of using these methods quickly becomes substantial when they are employed in design optimization where the same calculation may be repeated thousands of times.

### 5.1 Wing Design Variables

To develop and test the variable-complexity response surface optimization strategy we decided to construct an example problem involving only a few variables. For this reason, a four variable wing design problem was chosen. Here, two of the original planform variables, root chord and tip chord, were selected along with two new design variables (Fig. 5). The first new design variable was the inboard leading-edge sweep angle which was calculated from the original planform variables  $x_2$  and  $x_3$ . The second new variable is a constant scaling factor,  $\zeta$ , by which the three  $t/c$  ratios from the HSCT baseline were modified. For example,  $(t/c)_{root,new} = \zeta(t/c)_{root,baseline}$ ,  $(t/c)_{break,new} = \zeta(t/c)_{break,baseline}$ , and  $(t/c)_{tip,new} = \zeta(t/c)_{tip,baseline}$ , for  $0.8 \leq \zeta \leq 1.2$ . Thus, this new variable,  $\zeta$ , replaces the three  $t/c$  ratio design variables used in the original HSCT wing parameterization. In addition to the new variable definitions, planform variables  $x_4$  and  $x_5$  were eliminated so that the trailing edge of the wing was straight. Further, in this simplified model the span was held fixed.

Variations in the root chord have a significant effect on both the structural weight of the wing and on the volume available within the wing for fuel storage. These characteristics directly influence the gross weight of the HSCT. Perturbations in the leading-edge sweep and the  $t/c$  scaling factor primarily affect supersonic drag due to lift and the volumetric wave drag. Thus, the range and gross weight of the HSCT are affected through variations in the drag components.



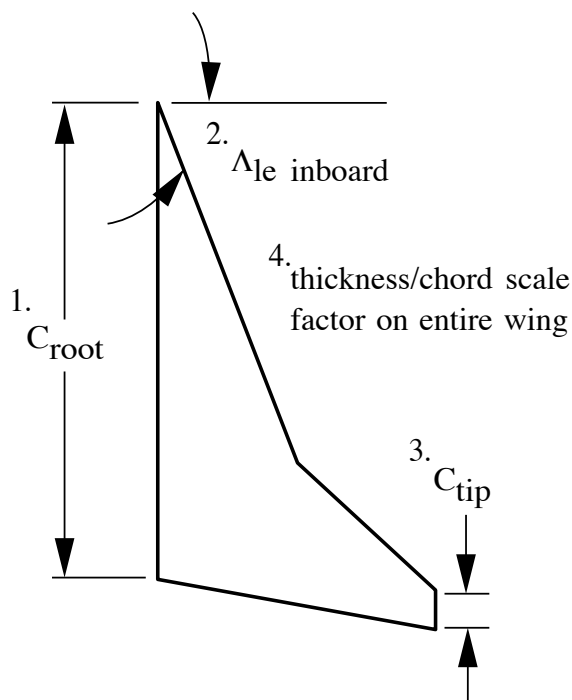


Figure 5. Wing design variable definition for the four variable problem.

The tip chord variable was selected specifically because it has only a minor impact on the weight and performance of the HSCT. For this reason, it was expected that the regression analysis and analysis of variance techniques would identify as negligible some of the response surface terms involving tip chord. This was confirmed by the analysis results and is discussed below. Note that although the tip chord is a relatively unimportant design variable for this example problem and the analysis methods used, the aerodynamics of the wing tip region can strongly influence the design of a particular aircraft. Therefore, the tip chord is not a design variable that can be ignored.

The design space for this four variable problem was determined by allowing the root chord and tip chord to vary  $\pm 20$  percent from the values on the baseline HSCT. The  $t/c$  scaling factor also varied  $\pm 20$  percent from a nominal value of unity. The leading-edge sweep was allowed to range only  $\pm 9$  percent from its baseline value. Variations in the sweep angle outside of this range produced configurations which were not realistic.

## 5.2 Design Space Reduction

The first stage in the variable-complexity response surface modeling process was to evaluate numerous HSCT designs using simple algebraic analysis methods. This was performed by discretizing the design space using a  $6 \times 6 \times 6 \times 6$  uniform coarse grid, i.e., each design variable had six discrete values. The 1,296 ( $6^4$ ) configurations defined by the combinations of the design variable values were then analyzed. At the center of the design space was the baseline HSCT configuration.

Using the constraint data obtained for each of the 1,296 HSCT designs, obvious “non-sense” configurations were eliminated from consideration. Here, designs were excluded if any of the aerodynamic/performance constraints (e.g., landing angle-of-attack  $\leq 12^\circ$ ) were violated by more than twenty percent, and if any geometric constraints (e.g., minimum airfoil chord lengths  $\geq 7$  ft.) were violated by more than five percent. In addition, gross

takeoff weight (GTOW) was allowed to vary within  $\pm 20$  percent of the baseline GTOW of approximately 650,000 lbs. and range was required to be greater than 5,000 *n.mi.* Both of these constraints were imposed to remove from consideration any unrealistic designs which had not been eliminated previously. After applying these constraints, only 157 acceptable HSCT designs remained out of the initial 1,296 designs.

### 5.3 Regression Analysis and ANOVA

Since range is directly affected by numerical noise in the supersonic drag due to lift and volumetric wave drag calculations, a response surface model for range was used to determine the reduced-term polynomial model for the *D*-optimal point selection and for later use in modeling the drag components. An alternative approach, and one that will be considered in our future work, would have been to apply regression analysis and ANOVA separately to response surface models for each of the drag components.

With the data from the 157 simple HSCT analyses a fifteen term polynomial response surface model was fit to the aircraft range data. Using the regression analysis and ANOVA methods described above, the coefficients of variation for the fifteen terms in the response surface model were calculated (Table 3). Here, the abbreviations  $\zeta$ ,  $c_r$ ,  $c_t$ , and  $\Lambda_{LE}$  correspond to the *t/c* scaling factor  $\zeta$ , root chord, tip chord, and leading-edge sweep angle, respectively. As shown, the higher order terms involving  $c_t$  have coefficients of variation greater than ten percent and can safely be dropped from the response surface model. Thus, the number of terms in the response surface model was reduced to eleven and the modeling of the tip chord variable was simplified from quadratic to linear.

Table 3. Regression analysis and ANOVA data for the range response surface model.

Variable	Coeff.	Std. Dev	V	Variable	Coeff.	Std. Dev	V
<i>const.</i>	0.058	0.197	3.416	$\zeta$	-1.200	0.268	0.224
$c_r$	-0.555	0.206	0.372	$c_t$	-0.054	0.133	2.443
$\Lambda_{LE}$	0.755	0.261	0.346	$\zeta c_r$	-0.221	0.627	2.835
$\zeta c_t$	0.009	0.372	40.616	$\zeta \Lambda_{LE}$	0.170	0.848	4.990
$c_r c_t$	-0.025	0.290	11.621	$c_r \Lambda_{LE}$	0.058	0.572	9.907
$c_t \Lambda_{LE}$	-0.021	0.358	16.955	$\zeta^2$	-0.095	0.623	6.588
$c_r^2$	-0.147	0.352	2.399	$c_t^2$	-0.006	0.234	42.143
$\Lambda_{LE}^2$	-0.107	0.700	6.526				

The accuracy of the response surface fit is only slightly impaired after removing terms from the polynomial model for which the coefficient of variation was large. With all fifteen terms in the polynomial, the average error (in nautical miles) was 11.71, the RMS error was 14.99 and the maximum error was 43.13. Removing four terms from the original polynomial brought the average error to 11.98, the RMS error to 15.45 and the maximum error to 38.61. Here, the errors are calculated from the difference between the response surface prediction for the range and the actual value for the range at each of the 157 remaining HSCT design points.

From the 157 HSCT designs, fifty were selected on the basis of the *D*-optimal criterion. The performance and constraint criteria for each of these were then evaluated using the detailed aerodynamic analysis models.

Using the same eleven term polynomial model found for range, new response surface models were constructed for the wave drag, the lift curve slope, and the leading-edge thrust term. These three response surface models were then used in the range calculation subroutine in place of the original noisy calculations of the drag components.

#### 5.4 Optimization Techniques

As described above, the optimization for the variable complexity response surface approximation method uses constraints based on both the simple and detailed analysis models. For the example problem, this is accomplished by using two constraints on the calculated range.

The approximate constraint uses the original range calculation, i.e., range calculated from the simple analysis of drag components, which must be greater than 5,000 *n.mi.* This is the same constraint used to remove unrealistic design points after the initial 1,296 HSCT analyses.

The new range constraint employs the smooth response surface models for the three drag components. This constraint stipulates that the range must be greater than 5,500 *n.mi.* The complication is that the range based on the response surface models is accurate only for certain regions of the design space defined by the allowable design variable values. One may picture the response surface models as being valid on a four-dimensional spheroid inscribed within a four-dimensional hypercube, where the vertices of the hypercube are defined by the allowable limits on the design variables. Without the approximate range constraint  $\geq 5,000$  *n.mi.*, the optimizer invariably moves to a vertex of the hypercube outside of the spheroid on which the response surface models are valid.

At first this seems counterproductive since two constraints are now used for range whereas only one sufficed before. However, this arrangement circumvents the problems created by numerical noise in the original range constraint evaluation. The use of both approximate and response surface based range constraints is successful because the simple, noisy range constraint is not active for much of the optimization. It serves only to keep the optimizer from moving to a region of the design space where the response surface model is inaccurate. In contrast, the response surface based smooth range constraint is nearly always active but it is not affected by numerical noise.

Due to improvements and corrections in various elements of our HSCT analysis software, the previously feasible baseline HSCT configuration, was found to slightly violate several constraints. In particular, these violated constraints pertained to takeoff and landing conditions regarding wing tip/runway scrape, engine/runway scrape, and landing angle-of-attack. Since span was not a design variable in this example problem, some of these constraints would have remained violated for all combinations of the four design variables. Therefore, to complete this investigation, the constraints in violation were removed, and the landing angle-of-attack constraint was relaxed from  $12^\circ$  to  $13^\circ$ . With the HSCT baseline configuration now providing a feasible starting point, optimization cases both with and without the response surface models for drag were conducted.

#### 5.5 Optimization Results

With the range constraint based on the response surface models for volumetric wave drag and the two components of supersonic drag due to lift, the NEWSUMT-A optimizer was used to determine the optimal combination of wing design variables to yield minimum gross weight while satisfying all constraints. The results of the optimization are shown in Table 4 in which the design variables and performance are compared for the initial and optimal HSCT configurations. Figure 6 shows the difference between the baseline HSCT planform from which the optimization was started and the optimal planform. The planform changes

for the optimal wing design are most noticeable in the length of the root chord and in the leading-edge sweep angle. However, these differences are relatively modest.

Table 4. HSCT performance data for the initial and optimal HSCT designs.

	<b>Initial</b>	<b>Optimal</b>		<b>Initial</b>	<b>Optimal</b>
root chord	174.0 <i>ft.</i>	171.1 <i>ft.</i>	Wing Weight	107,410 <i>lbs.</i>	103,123 <i>lbs.</i>
tip chord	8.1 <i>ft.</i>	7.8 <i>ft.</i>	Fuel Weight	328,044 <i>lbs.</i>	310,750 <i>lbs.</i>
LE sweep	71.88°	72.44°	GTOW	643,393 <i>lbs.</i>	620,876 <i>lbs.</i>
t/c scale	1.00	0.92	Fuel/Gross	50.99 %	50.05 %
Exact Range	5,577 <i>n.mi.</i>	5,510 <i>n.mi.</i>	$C_{D_{wave}}$	0.0017	0.0015
R.S. Range	5,546 <i>n.mi.</i>	5,519 <i>n.mi.</i>	Total Drag	0.0053	0.0052
Landing AOA	12.28°	12.33°			

The thinner wing results in a lower wave drag coefficient and thus a lower total drag coefficient. This improvement in aerodynamic efficiency permits the elimination of 18,000 *lbs.* of unneeded fuel. Additional weight savings occur because the optimal wing is smaller. Specifically, the wing area has decreased by 5.5 percent. Although the optimal wing is thinner, and therefore requires a heavier structure, the weight penalty is offset by the decrease in wing size. Thus, the optimal wing design results in a combined weight reduction of approximately 22,500 *lbs.*, which is a 3.5 percent decrease in GTOW.

For comparison, the optimization of the four variable design problem was repeated, but without using the response surface models for the drag components. In this case the sequential approximate optimization strategy was applied. The result of this optimization yielded a nearly identical optimal design as was obtained using the optimization with the response surface models. Differences in the optimal design variables and in the analysis results were negligible.

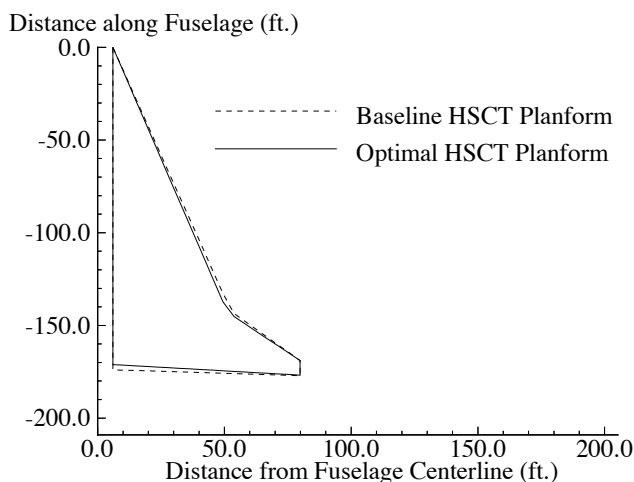


Figure 6. Baseline vs. optimal HSCT planforms.

In this case, the optimizer also found the minimum design after one sequential approximate optimization cycle. However, this was not unexpected since the baseline HSCT design was very close to an optimal design. In general, the optimal design will not be near the initial HSCT design and experience has shown that the sequential approximate optimization

strategy will require approximately twenty global optimization cycles until convergence is reached.

## 6 Wing Structural Weight Estimation

Gross takeoff weight is minimized during the HSCT configuration optimization process. Therefore, weight calculations are numerous and the final HSCT design is highly dependent on the accuracy of these results. To ease the computational expense of the design process, we have implemented the statistical weight equation in the weight module of Flight Optimization System (FLOPS) [24]. FLOPS is used to determine take-off gross weight and, more specially, to find the effect of planform geometry changes on structural weight. However, since the HSCT is a new aircraft, the weight equation does not account for all features of the design.

Because of the limitations within FLOPS, we have looked to improve upon the accuracy of the structural weight predictions. In particular, we have focused on the wing bending material weight since most of the load-dependent wing weight is due to bending.

### 6.1 The Weight Equation

The general wing weight equation in FLOPS is based on an analytic expression to relate wing bending material weight to wing geometry, material properties and loading. Other terms are added to account for shear material, control surfaces, etc. In addition, constants are included to correlate with a wide range of existing transports and reflect features such as composite materials, strut braced wings, etc. The wing weight,  $W_w$ , used within FLOPS is given as

$$(4) \quad W_w = \frac{W_g K_e W_b + W_s + W_n}{1 + W_b},$$

where

$$W_s = 0.68 (1 - 0.17f_c) (S - S_b)^{0.34} W_g^{0.6},$$

$$W_n = 0.35 (1 - 0.3f_c) S^{1.5},$$

$$W_b = K f_{ul} b (1 - 0.4f_c) (1 - .01f_a),$$

$$K = 8.8B_z \left(1 + (6.25/b)^{0.5}\right) \times 10^{-6},$$

$$K_e = 1.0 - (B_{ze}/B_e) (W_{pod}/W_g),$$

and  $W_g$  is the gross take-off weight (*lbs*),  $W_b$  is the wing bending material weight (*lbs*),  $W_s$  is the wing shear material and flaps weight (*lbs*),  $W_n$  is the wing control surfaces and non-structural weight (*lbs*),  $W_b$  is the wing bending material weight (*lbs*),  $W_{pod}$  is the engine pod weight (*lbs*),  $b$  is the wing span (*ft*),  $B_z$  is the bending material factor,  $B_{ze}$  is the engine relief factor,  $f_{ul}$  is the ultimate load factor,  $f_a$  is the composite material factor,  $f_c$  is the aeroelastic tailoring factor,  $S$  is the wing area ( $ft^2$ ), and  $S_b$  is the wing box area ( $ft^2$ ).

The FLOPS wing weight calculation is an iterative process since the wing weight and the gross take-off weight are dependent on one another. The system is closed except for the bending material factor,  $B_z$ , and the engine relief factor,  $B_{ze}$ .  $B_z$  accounts for the load distribution on the wing and is calculated by approximately determining the required material volume of the upper and lower skins in a simple wing box description of the wing.  $B_{ze}$  accounts for the reduced amount of structural weight necessary due to the presence of the engines on the wing.

## 6.2 Response Surface Approximation to Weight Equation

Finite-element based structural optimization appears to be an effective way to improve the estimate for the wing bending material weight given by FLOPS. However, finite-element solutions do not produce smooth functions with respect to the design variables. Thus, gradient-based optimizations are difficult to perform. In addition, the computational expense of finite-element solutions prevents them from being used frequently within the HSCT design optimization process. For these reasons, we have turned to a response surface approximation of the wing bending material weight. This provides a simple algebraic means of calculating accurate values for the wing bending material weight while at the same time giving smooth derivative information.

In the development of the response surface, a large number of data points, which span the design space, are required; however, we are limited by the expense of performing structural optimizations. For this reason, the wing bending material weight predicted by FLOPS will be used to develop the response surface. Once this is done, a sequence of structural optimizations will be performed using finite element analysis to generate the final form of the response surface.

## 6.3 The Model Equation

To determine a generalized model equation, we looked at the basic form of statistical weight equations such as those defined within FLOPS. A basic algebraic relationship which appears repeatedly is:

$$(5) \quad y = C x_1^{c_1} x_2^{c_2} \cdots x_n^{c_n},$$

where  $y$  is the objective function and  $x$  are the variables. From this a generalized model equation can be represented as:

$$(6) \quad \ln(y) = c_o + \sum_p 1 \leq i \leq p c_i \ln(x_i) + \sum_{1 \leq i \leq j \leq p} c_{ij} \ln(x_i x_j) + \delta,$$

Essentially, the logarithm of the response,  $y$ , is a function of a quadratic in the logarithms of the variables,  $x$ . The  $c_i$  coefficients are unknown values which must be found through the method of least squares.

## 6.4 Identification of the Feasible Design Space

For simplicity, we initially chose the variables to be twenty-five of the twenty-eight HSCT design variables. The remaining three variables, the wing leading edge radius, the cruise climb rate and the starting cruise altitude were neglected because they had no effect on the wing bending material weight. The enormous design space associated with the twenty-five variables, as well as the expense of performing structural optimizations, forced us to limit the response surface to feasible regions of the space. Therefore, the first step in the response surface design was to find a large group of candidate points in the feasible region.

Initially, we found a twenty-five dimensional hypercube which encompassed the entire feasible region. This was accomplished by allowing each of the variables to assume values between 20 percent and 180 percent of their baseline value, given in Table 1. In this response design space, 19,651 configurations were found distributed evenly throughout the hypercube. Of these designs, 83 percent violated one or more of the HSCT geometric constraints. Using a simple search method, each of the geometrically infeasible configurations

was moved into the feasible region of the design space by moving the design a distance  $\alpha$  closer to the baseline configuration.

$$(7) \quad \mathbf{x}' = \alpha(\mathbf{x} - \mathbf{x}_c) + \mathbf{x}_c$$

$\mathbf{x}'$  is the transformed point based on  $\mathbf{x}$  while  $\mathbf{x}_c$  is the baseline value discussed previously. To further limit the extent of the design space, obvious nonsense designs were removed based on the wing bending material weight predicted by FLOPS. Values below 20,000 *lbs.* or above 120,000 *lbs.* were considered unreasonable and excluded from the set of candidate points. Thus, we were left with 18,152 feasible designs.

### 6.5 Selection of Intervening Variables

Using the initial twenty-five variables and the 18,152 design points, a response surface model was fit to wing bending material weight estimates from FLOPS. The accuracy of this response surface, however, was found to be unacceptable. The average error was 952 *lbs.*, the RMS error was 2,895 *lbs.*, and the maximum error was 196,576 *lbs.* Errors were calculated from the difference between the response surface predictions for the wing bending material weight and the values predicted by FLOPS.

One method to find a more accurate response surface would be to use the same variables in conjunction with another form of the model equation. However, the quadratic equation was already very general and moving to a more general equation, like a cubic, would significantly increase the complexity of the model equation. For this reason we chose to find an alternative set of variables, intervening variables, which would be more appropriate for a weight analysis while also being entirely dependent on the design variables. Compared to the original variables, properly chosen intervening variables can produce accurate results using a less complex model equation.

Returning to the description of the FLOPS weight equation, the wing weight is based on a set of ten basic parameters. Listed in Table 5, each of these parameters can be found using the twenty-five HSCCT design variables. Using these terms as the intervening variables produced dramatically better results. The average error was 17 *lbs.*, the RMS error was 47 *lbs.*, and the maximum error was 1,345 *lbs.*

Table 5. Basic parameters used to calculate wing weight in FLOPS.

Num.	Name	Description	Num.	Name	Description
1	$S_{ht}$	Horiz. tail area	6	$B_{ze}$	Engine relief factor
2	$S_{vt}$	Vert. tail area	7	$B_z$	Bending material fact.
3	$wfuse$	Max. fuselage diam.	8	$S_w$	Wing surface area
4	$b$	Wing span	9	$W_{fuel}$	Takeoff fuel weight
5	$sweep$	Ave. 1/4 chord sweep	10	$W_{to}$	Gross weight from FLOPS

### 6.6 Regression Analysis and ANOVA

The FLOPS weight equation was used to find the wing bending material weight for the 18,152 designs. Using these values as the objective function and the ten intervening variables discussed previously, regression analysis and analysis of variance (ANOVA) methods were used to find the coefficients of variation for each of the sixty-six terms in the model equation. The non-linear terms with the lowest coefficient of variation were then removed from the model equation, and the process of regression analysis and ANOVA was repeated.

Figure 7 shows the accuracy of the response surface compared to the number of terms remaining in the model equation. Reducing the complexity of the model equation by forty-one terms had only a minor impact on the accuracy. This twenty-five term model equation was chosen for further analysis.

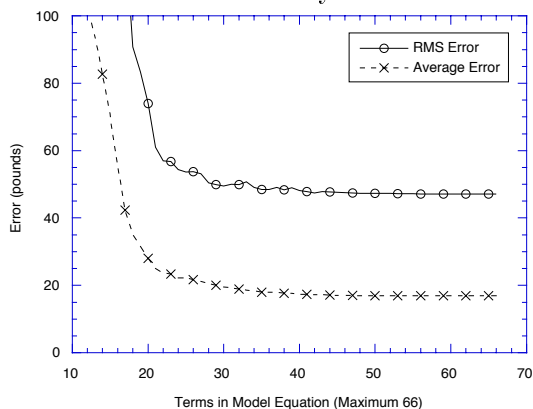


Figure 7. RMS Error versus terms remaining in the model equation.

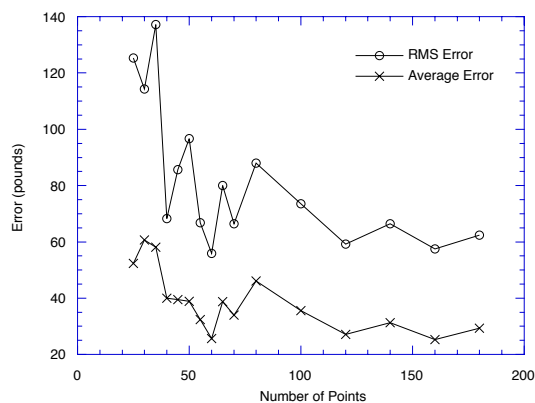


Figure 8. Comparison of the twenty-five term model equation accuracy using *D*-Optimal points.

Up to this point, all 18,152 configurations had been used to construct the response surface. However, the expense of structural optimizations severely limits the number of designs which can be considered. To address this issue, several subsets of the 18,152 points were identified using *D*-optimality [3]. The accuracy of the model equation versus the number of design points used is given in Figure 8. As with the number of terms in the model equation, the number of points required to produce an accurate response surface is significantly less than the original 18,152 points. From Figure 8, it appeared that sixty configurations would produce an accurate response surface based on the twenty-five term model equation.

## 6.7 Structural Optimization

The structural optimization procedure minimizes the weight for a given fixed arrangement of the spars and ribs with the thicknesses of skin panels, spar and rib cap areas as design variables. Von Mises stress constraints are applied to all the panel, spar, and rib cap elements. Local buckling constraints are also applied.

Creating a response surface requires numerous planform evaluations. For this reason, a special mesh generator was implemented to automatically create a finite element model based on the 28 HSC T design variables. In addition to design variables, the number of frames in the fuselage, the number of spars and ribs in the wing and the chord fractions taken by the leading and trailing edge control surfaces must be specified. The mesh generator creates the finite element nodes and element topology data in addition to estimating the location of non-structural weights and the geometry of the wing fuel tanks [17].

A typical finite element model is made up of 923 elements joined at 193 nodes with 579 total degrees of freedom. The wing and fuselage skin are modeled by membrane elements. Spar and rib cap elements are modeled by rod elements. Vertical rods and shear panels are used to model spar and rib webs. The initial thicknesses and areas of the elements were chosen to match the estimated structural weight. The aircraft is assumed to be built of titanium. Because of symmetry, only half of the aircraft was modeled.



The loads applied to the structural model are composed of the aerodynamic forces and inertia forces due to the distributed weight of the structure, non-structural items and fuel. Aerodynamic loads for supersonic flight conditions were determined using a supersonic panel method, and loads for subsonic flight conditions were from a vortex-lattice method. Carlson's WINGDES program was used to generate a cambered wing from the given aerodynamic configuration [5]. The loads at the aerodynamic nodes were mapped to the structural nodes using surface spline interpolation. The structure was assumed to be rigid for the determination of aerodynamic forces. (Previous studies indicated that structural flexibility did not have a large effect on the loads for this particular configuration [1], [18].) The fuel was assumed to be stored in thirty-one tanks throughout the aircraft. More details about load cases used can be found in [20].

## 7 Parallel Computing

### 7.1 Parallel Implementation of Aerodynamic Analysis

Our efforts at parallel computing involve a twenty-eight node Intel Paragon at Virginia Tech. The coarse grained parallelization of the aerodynamic analysis modules within the full HSCT analysis code makes use of a master-slave paradigm on the Paragon whereby one designated master node controls the data transfer and file input/output (I/O) of the remaining slave nodes. This coarse grained approach is used for the numerous independent analyses required for response surface construction.

To initiate the parallel multipoint analyses, a group of predetermined analysis points is input to the master node. The master node then computes the subset of the points which each slave node will analyze and sends that information to the appropriate slave. Both the master and slave nodes then analyze their respective subsets of the selected points and store the results in an array local to each node. When each slave has finished its portion of the analyses, it sends the array of analysis values to the master node for output.

To compare the computational savings for parallel versus serial execution of a code, the term *speedup* is defined as  $T_s/T_p$ , where  $T_s$  is the serial execution time and  $T_p$  is the parallel execution time using  $p$  processors. Figure 9 shows the speedup results for parallel execution of the HSCT analysis code compared to ideal, linear speedup. The actual results deviate from the ideal due to the file I/O demands of the analysis code which must be executed serially, and due to unavoidable communication overhead in the parallel code. Currently we are examining methods to reduce file I/O and improve the parallel execution of the HSCT analysis code. Our efforts to date are detailed in Reference [4].

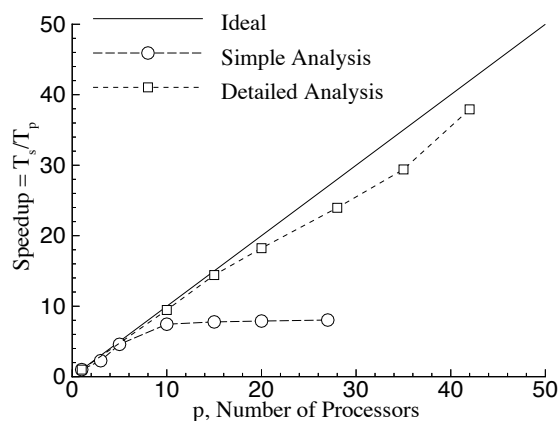


Figure 9. Ideal versus actual speedup for parallel execution of the HSCT aerodynamic code.

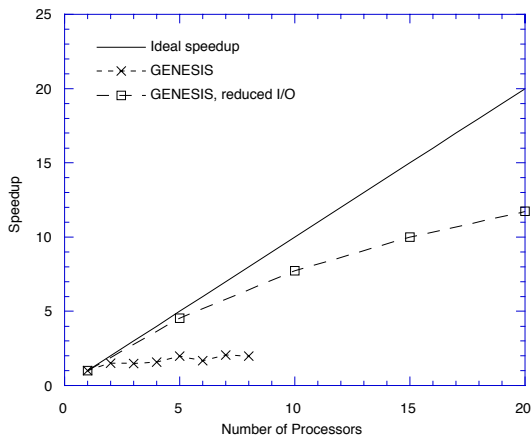


Figure 10. Ideal versus actual speedup for parallel execution of the GENESIS code.

## 7.2 Parallel Implementation of Structural Analysis

The repeated structural optimizations required to produce a response surface are suitable for coarse-grained parallel computation. Coarse-grained parallelization implies that multiple configuration geometries will be evaluated simultaneously, each on a separate processor. There is no interaction between the processors, each maintaining their own input and output data.

For a distributed memory architecture, disk I/O limits the efficiency of the parallel computations as the number of processors are increased. This factor was the primary basis for choosing a particular structural optimization code to implement in the parallel environment. GENESIS, a finite-element structural optimization code developed and supported by Vanderplaats, Miura and Associates, Inc [11], was available from the developer in a reduced I/O form and thus made it an effective code to use on the Paragon. With the standard version of GENESIS the maximum speedup level is 2.3 even with a large number of processors. The reduced I/O version achieves a speedup of 11.7 using twenty processors (Fig. 10).

## 8 Continuing Work

Currently the four variable HSCT wing design problem is being fully explored and the variable-complexity response surface modeling techniques are being refined. These methods will be applied to a new HSCT design problem involving seven to ten design variables to further validate the response surface modeling procedure.

We have developed a model equation which has been found to be effective in predicting the wing bending material weight given by the FLOPS weight equation. Our future efforts focus on evaluating the suitability of the model equation to data produced by GENESIS. This will be accomplished by performing numerous structural optimizations in parallel for a subset of the 18,152 planforms generated previously. The subset of points will be determined using the  $D$ -optimal criterion and the objective will be to find the minimum number of points required to produce an accurate response surface model.

The final form of the response surface model, based on the finite element structural optimizations, will be integrated into the HSCT design process. The algebraic response

surface model will replace the wing bending material weight term calculated using FLOPS. One problem which we anticipate will be identifying regions where the response surface is inaccurate. The optimizer may evaluate designs outside of the domain of validity for the response surface and would calculate erroneous values for the wing bending material weight. To circumvent this problem, an additional constraint will be added to the optimizer which will preclude HSCT designs where the FLOPS equation predicts a wing bending material weight outside of the range used to create the response surface. This fits into the variable-complexity modeling strategy in that the inexpensive FLOPS evaluations are used in conjunction with the response surface models calculated from the GENESIS finite element optimizations.

## 9 Concluding Remarks

A variable-complexity response surface modeling strategy has been developed and has been applied to the multidisciplinary design optimization of an HSCT. The feasibility of this method has been demonstrated using response surface models for aerodynamic drag components in a four variable HSCT wing design problem. Further, the response surface techniques have been applied to structural analysis in the development of a model for the wing bending material weight for various HSCT configurations. This structural model will be integrated into the overall HSCT design optimization framework. The combined variable-complexity aerodynamic and structural response surface methods will then be applied to the full HSCT design problem involving twenty-eight or more design variables. Additional efforts will be directed at further improving the parallel performance of both the aerodynamic and structural analysis methods.

## References

- [1] Barthelemy, J. F. M., Wrenn, G. A., Dovi A. R., Coen, P. G., and Hall, L. E., *Supersonic Transport Wing Minimum Weight Design Integrating Aerodynamics and Structures*, J. of Aircraft, vol. 31, No. 2, March–April 1994.
- [2] Box, G. E. P. and Behnken, D. W., *Some New Three Level Designs for the Study of Quantitative Variables*, Technometrics, vol. 2, No. 4, November, 1960, pp. 455–475.
- [3] Box, M. J. and Draper, N. R., *Factorial Designs, the  $|\mathbf{X}^T\mathbf{X}|$  Criterion, and Some Related Matters*, Technometrics, vol. 13, No. 4, 1971, pp. 731–742.
- [4] Burgee, S., Giunta, A. A., Narducci, R., Watson, L. T., Grossman, B., and Haftka, R. T., *A Coarse Grained Variable-Complexity Approach to MDO for HSCT Design in Parallel Processing for Scientific Computing*, Bailey, D. H., Bjørstad, P. E., Gilbert, J. R., Mascagni, M. V., Schreiber, R. S., Simon, H. D., Torczon, V. J., and Watson, L. T. (eds.), SIAM, Philadelphia, PA, 1995, pp. 96–101.
- [5] Carlson, H. W., and Mack, R. J., *Estimation of Leading-Edge Thrust for Supersonic Wings of Arbitrary Planforms*, NASA TP-1270, 1978.
- [6] Carlson, H. W., Mack, R. J., and Barger, R. L., *Estimation of Attainable Leading-Edge Thrust for Wings at Subsonic and Supersonic Speeds*, NASA TP-1500, 1979.
- [7] Carlson, H. W., and Miller, D. S., *Numerical Methods for the Design and Analysis of Wings at Supersonic Speeds*, NASA TN D-7713, 1974.
- [8] Dudley, J., Huang, X., MacMillin, P. E., Grossman, B., Haftka, R. T., and Mason, W. H., *Multidisciplinary Optimization of the High-Speed Civil Transport*, AIAA Paper 95–0124, 1995.
- [9] Dudley, J., Huang, X., Haftka, R. T., Grossman, B., and Mason, W. H., *Variable-Complexity Interlacing of Weight Equation and Structural Optimization for the Design of the High Speed Civil Transport*, AIAA Paper 94–4377, 1994.

- [10] Englund, W. C., Stanley, D. O., Lepsch, R. A., McMillin, M. M., and Unal, R., *Aerodynamic Configuration Design Using Response Surface Methodology Analysis*, AIAA Paper 93-3967, Aug. 1993.
- [11] *GENESIS*, User Manual, Version 1.3, Dec. 1993.
- [12] Giunta, A. A., Dudley, J. M., Narducci, R., Grossman, B., Haftka, R. T., Mason, W. H., and Watson, L. T., *Noisy Aerodynamic Response and Smooth Approximations in HSCT Design*, AIAA Paper 94-4376, 1994.
- [13] Grandhi, R. V., Thareja, R., and Haftka, R. T., *NEWSUMT-A: A General Purpose Program for Constrained Optimization Using Constraint Approximation*, ASME J. Mechanisms, Transmissions and Automation in Design, vol. 107, 1985, pp. 94-99.
- [14] Harris, R. V., Jr., *An Analysis and Correlation of Aircraft Wave Drag*, NASA TM X-947, 1964.
- [15] Healy, M. J., Kowalik, J. S., and Ransay, J. W., *Airplane Engine Selection by Optimization on Surface Fit Approximations*, J. Aircraft, vol. 12, No. 7, 1975, pp. 593-599.
- [16] Hinkelman, Klaus., *Design and Analysis of Experiments*, John Wiley & Sons, Inc., 1994.
- [17] Huang, X., *Structural Optimization and its Interaction with Aerodynamic Optimization for a High Speed Civil Transport*, Ph.D. Dissertation, VPI&SU, November 1994.
- [18] Huang, X., Haftka, R. T., Grossman, B., and Mason, W., *Comparison of Statistical-based Weight Equations with Structural Optimization for Supersonic Transport Wings*, AIAA 94-4379, 1994.
- [19] Hutchison, M. G., *"Multidisciplinary Optimization of High-Speed Civil Transport Configurations Using Variable Complexity Modeling"*, Ph.D. Dissertation, VPI&SU, March 1993.
- [20] Hutchison, M. G., Huang, X., Mason W. H., Haftka, R. T., and Grossman, B., *Variable-Complexity Aerodynamic-Structural Design of a High-Speed Civil Transport Wing*, 4th AIAA/USAF/NASA/OAISymposium on Multidisciplinary Analysis and Optimization, Cleveland, OH, Sept. 21-23, 1992.
- [21] Hutchison, M. G., Unger, E. R., Mason, W. H., Grossman, B., and Haftka, R. T., *Aerodynamic Optimization of an HSCT Wing Using Variable-Complexity Modeling*, AIAA 93-0101, Jan. 1993.
- [22] Hutchison, M. G., Unger, E. R., Mason, W. H., Grossman, B., and Haftka, R. T., *Variable-Complexity Aerodynamic Optimization of an HSCT Wing Using Structural Wing-Weight Equations*, J. Aircraft, vol. 31, No. 1, 1994, pp. 110-116.
- [23] Mason, R. L., Gunst, R. F., and Hess, J. L., *Statistical Design and Analysis of Experiments*, John Wiley & Sons, New York, N. Y., 1989, pp. 215-221.
- [24] McCullers, L. A., *Aircraft Configuration Optimization Including Optimize Flight Profiles*, Proceedings of a Symposium on Recent Experiences in Multidisciplinary Analysis and Optimization, J. Sobieski, compiler, NASA CP-2327, April 1984, pp. 395-412.
- [25] Narducci, R., Grossman, B., and Haftka, R. T., *Sensitivity Algorithms for an Inverse Design Problem Involving a Shock Wave*, AIAA Paper 94-0096, Jan. 1994, to appear in Inverse Problems in Engineering.
- [26] Unger, E. R., Hutchison, M. G., Rais-Rohani, M., Haftka, R. T., and Grossman, B., *Variable-Complexity Design of a Transport Wing*, Intl. J. Systems Automation: Res. and Appl. (SARA), No. 2, 1992, pp. 87-113.